

Elisabete Aramendi, Andoni Elola, Erik Alonso, Unai Irusta, Mohamud Daya, James K. Russell, Pia Hubner, Fritz Sterz. Feasibility of the capnogram to monitor ventilation rate during cardiopulmonary resuscitation. *Resuscitation*, Volume 110, 2017, Pages 162-168, ISSN 0300-9572, <https://doi.org/10.1016/j.resuscitation.2016.08.033>.

(<https://www.sciencedirect.com/science/article/pii/S0300957216304725>)

Abstract

Aim

The rates of chest compressions (CCs) and ventilations are both important metrics to monitor the quality of cardiopulmonary resuscitation (CPR). Capnography permits monitoring ventilation, but the CCs provided during CPR corrupt the capnogram and compromise the accuracy of automatic ventilation detectors. The aim of this study was to evaluate the feasibility of an automatic algorithm based on the capnogram to detect ventilations and provide feedback on ventilation rate during CPR, specifically addressing intervals where CCs are delivered.

Methods

The dataset used to develop and test the algorithm contained in-hospital and out-of-hospital cardiac arrest episodes. The method relies on adaptive thresholding to detect ventilations in the first derivative of the capnogram. The performance of the detector was reported in terms of sensitivity (SE) and Positive Predictive Value (PPV). The overall performance was reported in terms of the rate error and errors in the hyperventilation alarms. Results were given separately for the intervals with CCs.

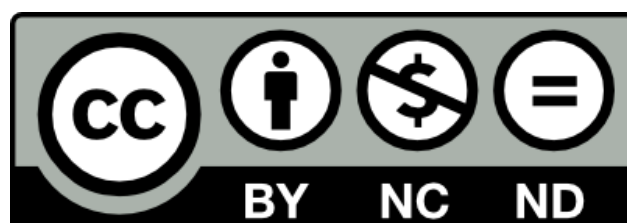
Results

A total of 83 episodes were considered, resulting in 4880 min and 46,740 ventilations (8741 during CCs). The method showed an overall SE/PPV above 99% and 97% respectively, even in intervals with CCs. The error for the ventilation rate was below 1.8 min⁻¹ in any group, and >99% of the ventilation alarms were correctly detected.

Conclusion

A method to provide accurate feedback on ventilation rate using only the capnogram is proposed. Its accuracy was proven even in intervals where capnography signal was severely corrupted by CCs. This algorithm could be integrated into monitor/defibrillators to provide reliable feedback on ventilation rate during CPR.

Keywords: Capnography, Ventilation monitoring, Cardiopulmonary resuscitation, Hyperventilation



Feasibility of the capnogram to monitor ventilation rate during cardiopulmonary resuscitation

Elisabete Aramendi^{*,a}, Andoni Elola^a, Erik Alonso^b, Unai Irusta^a, Mohamud Daya^c, James K.
Russell^c, Pia Hubner^d, Fritz Sterz^d

Affiliation and addresses:

^a Communications Engineering Department.
University of the Basque Country UPV/EHU.
Alameda Urquijo S/N
48013 Bilbao, Spain

^b Department of Applied Mathematics.
University of the Basque Country UPV/EHU.
Rafael Moreno "Pitxitxi", 3
48013 Bilbao, Spain

^c Department of Emergency Medicine.
Oregon Health & Science University.
97239-3098 Portland, OR, United States

^d Department of Emergency Medicine.
Medical University of Vienna.
1090 Wien, Austria

Word counts: 3110

Abstract: 257

Abstract

Aim: The rates of chest compressions (CCs) and ventilations are both important metrics to monitor the quality of cardiopulmonary resuscitation (CPR). Capnography permits monitoring ventilation, but the CCs provided during CPR corrupt the capnogram and compromise the accuracy of automatic ventilation detectors. The aim of this study was to evaluate the feasibility of an automatic algorithm based on the capnogram to detect ventilations and provide feedback on ventilation rate during CPR, specifically addressing intervals where CCs are delivered.

Methods: The dataset used to develop and test the algorithm contained in-hospital and out-of-hospital cardiac arrest episodes. The method relies on adaptive thresholding to detect ventilations in the first derivative of the capnogram. The performance of the detector was reported in terms of Sensitivity (SE) and Positive Predictive Value (PPV). The overall performance was reported in terms of the rate error and errors in the hyperventilation alarms. Results were given separately for the intervals with CCs.

Results: A total of 83 episodes were considered, resulting in 4880 min and 46740 ventilations (8741 during CCs). The method showed an overall SE/PPV above 99% and 97% respectively, even in intervals with CCs. The error for the ventilation rate was below 1.8 min^{-1} in any group, and $> 99\%$ of the ventilation alarms were correctly detected.

Conclusion: A method to provide accurate feedback on ventilation rate using only the capnogram is proposed. Its accuracy was proven even in intervals where capnography signal was severely corrupted by CCs. This algorithm could be integrated into monitor/defibrillators to provide reliable feedback on ventilation rate during CPR.

Keywords

Capnography, Ventilation monitoring, Cardiopulmonary resuscitation, Hyperventilation

1. INTRODUCTION

Quality of cardiopulmonary resuscitation (CPR) is a key factor in the outcome of cardiac arrest patients. Advanced life support (ALS) treatment of out-of-hospital cardiac arrest (OHCA) includes good-quality chest compressions (CCs) and a reliable airway management. The 2015 resuscitation guidelines recommend continuous chest compressions after intubation, ventilation rates of 10 min^{-1} and avoidance of hyperventilation.¹ Hyperventilation increases intrathoracic pressure, reshapes the oxygen dissociation curve (increasing oxygen affinity) and behaves as a cerebral vasoconstrictor.^{2,3} It has also been proven to lower coronary perfusion pressure and to contribute to hemodynamic deterioration in animal experiments.⁴⁻⁸ All these factors decrease the probability of survival.^{9,10} Nevertheless rescuers providing pre-hospital CPR often exceed the recommended ventilation rates. Several studies report rates ranging from moderate (14 min^{-1}) to severe ($> 20 \text{ min}^{-1}$) hyperventilation during long duration OHCA.^{5-7,9-12}

CPR feedback systems, either standalone or incorporated into defibrillators, have been shown to improve adherence to guideline recommendations.^{13,14} Feedback on CCs based on acceleration, force or thoracic impedance (TI) has been extensively studied;^{11,15-17} but little attention has been given to feedback on ventilation rate during CPR. The TI channel, recorded through the defibrillation pads, has been explored to monitor ventilation rate.^{11,18,19} However, an analysis of long resuscitation episodes showed that artefacts limit the reliability of TI for instantaneous feedback on ventilation rate.¹⁷ Currently, no commercial system is available for feedback on ventilation rate using the TI.

The recently released resuscitation guidelines have placed an increased emphasis on the use of the capnogram during CPR to monitor, among other things, ventilation rate and to avoid hyperventilation.¹ During CPR compression artefacts often corrupt the capnogram compromising the accuracy of automatic algorithms for ventilation rate feedback.²⁰⁻²² Few such algorithms have been published,^{23,24} and their performance during CPR has not been systematically evaluated and/or documented.

This study proposes an automatic algorithm for ventilation detection during CPR based on the typical waveform characteristics of the capnogram and on the use of adaptive thresholds to identify ventilations. The aim of the study is to analyse the feasibility of using the capnogram to provide an accurate automated feedback on ventilation rate and hyperventilation alarms during CPR.

31 **2. MATERIALS AND METHODS**

32 *2.1. Data materials*

33 Two datasets of episodes with signals from monitor/defibrillators were used in this study, an
34 out-of-hospital dataset (OHD) and an in-hospital dataset (IHD). The OHD was recorded during
35 cardiac arrest, with manual CPR (CCs and ventilations) provided in all episodes. The signals
36 available to monitor ventilations were the TI and the capnogram. The IHD corresponded to
37 patients who suffered cardiac arrest, some recorded during manual CPR (CCs and ventilations)
38 and some recorded after cardiac arrest during postresuscitation care (mechanical ventilation). They
39 were monitored with the capnogram and the expired air flow.

40 The OHD was a subset of a large OHCA registry containing 623 episodes maintained by the
41 Tualatin Valley Fire & Rescue (Tigard, Oregon, USA), an ALS first response agency. The episodes
42 were collected using the HeartStart MRx monitor/defibrillator (Philips, Andover, MA) between
43 2006 and 2009. Ventilations in these episodes were provided manually with an endotracheal tube or
44 laryngeal tube airway. Episodes with at least 20 minutes of concurrent and readable recordings of
45 the compression depth (CD), the TI and the capnogram were included in this study, resulting in a
46 dataset of 62 episodes. The CD signal from the Q-CPR assist pad by Philips was used to identify the
47 intervals with CCs. The capnogram was acquired using Microstream (sidestream acquisition) with
48 a sampling rate of 40/125 Hz and a resolution of 0.004 mmHg per bit. The instants of ventilations
49 were marked in the TI ventilation channel,^{11,17} first automatically and then manually reviewed
50 by three experienced biomedical engineers. Reviewers used the capnogram to make a decision in
51 unclear intervals. Fig. 1 shows examples of two episodes of the OHD, where ventilations are visible
52 in both the TI ventilation channel (in black) and the capnogram, for an artefact free interval (panel
53 a), and when CCs were provided (panel b).

54 The IHD was a subset of the APACHI study conducted by Philips Healthcare at the Medical
55 University of Vienna between November 2012 and January 2014. The APACHI study recorded
56 physiological signals (arterial blood pressure, electrocardiogram, photoplethysmogram, capnogram
57 and airway flow and pressure) from multiple monitors during hemodynamic crisis in the emergency
58 department of the Vienna General Hospital, under the direction of Drs. Sterz and Hubner. From
59 a total of 50 patients enrolled in the trial, the 21 that suffered cardiac arrest and had concurrent
60 recordings of capnogram and ventilatory flow were included. Six of the episodes were recorded

61 during CPR and 15 after resuscitation. The mainstream capnogram was acquired by the NICO
62 7300 monitor using the Capnostat CO₂ sensor by Philips (-125/125 L/min, 4 mV/L/min, 100
63 Hz). The respiratory signals were acquired by the same monitor; the airflow and the air volume
64 signals were used as gold standard (GS) to annotate the ventilations. Fig. 1 shows examples of
65 two episodes of the IHD, where ventilations are visible in the air volume and the capnogram, for
66 an artefact free interval (panel c) and when CCs were provided (panel d).

67 2.2. Ventilation detector

68 An automated algorithm that detects ventilations in the capnogram was developed based on
69 the four basic phases of a normal capnogram shown in Fig. 2: the inspiration baseline (phase I), the
70 expiration upstroke (phase II), the expiratory plateau (phase III) and the expiration downstroke
71 (phase IV).

72 The capnogram was first low-pass filtered to remove spectral components above 10 Hz, and
73 then a value of 5 mmHg was adopted as baseline. The inspiration (t_{insp}) and expiration (t_{exp})
74 times of potential ventilations were automatically detected from positive and negative peaks in the
75 first difference of the signal. For every potential ventilation the five features shown in Fig. 2 were
76 computed:

- 77 • Duration of the inspiration baseline, D_{insp} , in seconds.
- 78 • Mean CO₂ value of the inspiration baseline, A_{insp} , in mmHg.
- 79 • Mean CO₂ value of the expiratory plateau, A_{exp} , in mmHg.
- 80 • Area of the first second of the expiratory plateau, S_{exp} , in mmHg · s⁻¹.
- 81 • Relative CO₂ increase, $A_r = \frac{A_{exp} - A_{insp}}{A_{exp}}$.

The ventilation detector consists of a feature based decision algorithm which detects ventilations
by comparing D_{insp} and the minimum distance between ventilations with a fixed threshold value
(0.3s and 1.5s respectively) and features A_{exp} , S_{exp} and A_r with adaptive thresholds based on the
last p ventilations as follows:

$$Th_k = \frac{w}{p} \cdot \sum_{n=k-p}^k x_n \quad (1)$$

82 where Th_k is the adaptive threshold for k -th potential ventilation, w is a weighting factor between
83 0 and 1, and x_n represents the value of the feature for ventilation n .

84 A more detailed technical description of the algorithm is supplied in the Appendix A, where
85 signal processing techniques and ventilation detection criteria for the decision algorithm are
86 supplied. Two illustrative examples are also included to provide intermediate results that clarify
87 the implementation of the algorithm.

88 *2.3. Instantaneous ventilation rate and hyperventilation alarm*

89 The instants of ventilations detected in the capnogram were used to compute the ventilation rate
90 and to report hyperventilation alarms when an established rate was exceeded. Both measures could
91 be used to give real-time feedback to the rescuer. The instantaneous ventilation rate was computed
92 every 15s as the inverse of the median interval between ventilations in the previous minute.
93 Hyperventilation was defined for rates exceeding 15 min^{-1} , following the criteria established by
94 Kramer Johansen et al.¹³

95 *2.4. Evaluation and statistical analysis*

96 The episodes of the OHD were randomly allocated to training and test sets. The ventilation
97 detector was developed with the training set of the OHD, and evaluated with OHD test set and
98 the complete IHD. Results are given separately for intervals with and without CCs. All the results
99 were reported as median (interquartile range, IQR), as data did not pass the Anderson-Darling
100 normality test.

101 The performance of the ventilation detector was evaluated in terms of Sensitivity (SE), the
102 proportion of correctly detected ventilations, and Positive Predictive Value (PPV), the proportion
103 of detected ventilations corresponding to real ventilations.

104 The Concordance Correlation Coefficient (CCC) was reported in order to quantify the
105 agreement between the ventilation rate calculated from the GS and from the algorithm. The
106 percentage of ventilation rate errors $> 2 \text{ min}^{-1}$ per episode were reported. Bland-Altman plots
107 were used to show the level of agreement (95% LOA) between the algorithm and the GS.

108 The performance of the hyperventilation detector was evaluated in terms of correctly detected
109 hyperventilation alarms and the number of false hyperventilation alarms.

110 3. RESULTS

111 Table 1 summarizes the main characteristics of the datasets. For the 62 episodes of the OHD
112 the duration was 38 (34-46) min, the median ventilation rate per episode was 9.9 (8.7-13.1) min^{-1}
113 and the hyperventilation fraction per episode was 10 (2-35)%. For the 21 episodes of the IHD the
114 duration was 91 (50-141) min, the median ventilation rate per episode was 14.3 (12.6-18.2) min^{-1}
115 with 14 (0-88)% of hyperventilation fraction.

116 The OHD episodes were allocated randomly to training (37) and test sets (25). Fig. 3 shows
117 the boxplot of the performance of the ventilation detector for both the OHD and IHD datasets.
118 The SE was above 99% and the PPV above 97% overall. The boxplots show a slight deterioration
119 for the intervals during CCs. The median SE and PPV decreased at most one point during CCs,
120 and the lower quartile between 1 and 7 points.

121 Fig. 4 shows four examples where the dashed lines represent ventilations annotated in the GS
122 and the red triangles represent the ventilations detected by the algorithm. Panels a and b show two
123 examples of OHD where ventilations were missed due to too short inspiration intervals (panel a)
124 and because of the 'shark fin' waveform of the capnogram (panel b). Panels c and d show intervals
125 of the OHD and IHD, where the ventilations were correctly identified despite severe CC artefacts.

126 The concordance between the instantaneous ventilation rate obtained from the GS and from
127 the algorithm was high ($\text{CCC} > 0.98$) for the two datasets, even during CCs. The proportion of
128 errors larger than $> 2 \text{ min}^{-1}$ were 0 (0-4.2)% per episode for the OHD and 0 (0-1.2)% for the IHD.
129 Fig. 5 shows the Bland-Altman plots and the 95% LOA between the GS and the algorithm, which
130 was in all cases smaller than 1.8 min^{-1} .

131 For the OHD, the algorithm correctly detected 841 of 860 alarms, and 26 of the 867 given
132 alarms were false. For the IHD, the hyperventilation detector correctly reported 3563 of the 3566
133 hyperventilation alarms, and 12 of the 3575 given were false.

134 4. DISCUSSION

135 This study proposes an automatic algorithm to detect ventilations using the capnogram, and
136 thoroughly tests its accuracy for ventilation rate feedback during CPR, specifically addressing
137 intervals in which CCs were delivered. The algorithm identifies the instants of ventilations based
138 on adaptive thresholds to accommodate to the time-varying levels of CO₂, and avoids the rapidly
139 changing artefacts added by the CCs. This algorithm would permit an accurate ventilation rate
140 monitoring and a better control of hyperventilation both in- and out-of-hospital, where rates
141 recommended by resuscitation guidelines are frequently exceeded.^{5-7,9-12}

142 4.1. The dataset and the gold standard

143 The dataset used in this study includes both in-hospital and OHCA episodes, with a total
144 of 46740 ventilations (8741 during CCs). In the OHD impedance was used as gold standard, and
145 annotations were reviewed with the capnogram, but only in unclear intervals (see panel a of Fig. 4).
146 This procedure, which was a standard practice in previous studies because no better gold standard
147 is available for the OHCA data,²³ might limit the validity of the results. In order to overcome this
148 limitation an independent GS, not available in the OHCA setting, was introduced in the IHD, the
149 airway flow signal which provides reliable information for ventilation monitoring.^{1,23} In our IHD
150 the airway flow and volume signals from the NICO respiratory monitor by Philips were used as GS.
151 The number of episodes in our IHD is small, however this dataset contains the most reliable GS
152 used to date to validate capnogram based ventilation detectors during cardiac arrest. The results
153 obtained with this dataset confirmed the accuracy observed for the ventilation detection algorithm
154 with the OHCA dataset.

155 The global SE/PPV of the detector were 0.7/2.8 points better for the IHD than for the OHD
156 (Fig. 3), which may reflect various factors. On the one hand, the capnography technique was
157 different in our two datasets, mainstream for the IHD and sidestream for the OHD.²⁵ In mainstream
158 capnography the sensor is located directly in the way of the expired flow. In sidestream capnography
159 a sample of the patient's expired gases is transported to the sensor site using a 1-2 meter long tube.
160 This produces a delay in the capnogram with respect to the TI (4 seconds in our data) and the
161 diffusion of the gases during transport lowers the slopes (dampening) of the capnogram.²⁶ This last
162 effect might jeopardize the discrimination of ventilations in the OHD, as the algorithm is based on
163 the detection of abrupt changes in the capnogram, and might partially explain the lower accuracy

164 obtained for the OHD dataset. On the other hand, the OHD reflects more challenging scenarios
165 in which ventilations were manual and CPR was delivered in most of the cases, while 15 of the 21
166 in-hospital cases were mechanically ventilated and/or had no CCs. However, when cases during
167 CPR were considered the results were similar for the OHD and IHD (see Fig. 3 during CPR).
168 This primarily is because during CPR both datasets reflected the effects of greater variability in
169 ventilation patterns, CC artefacts and the intervention of multiple rescuers. The results for the
170 IHD data with a reliable and independent GS confirm the observations on the larger OHD, and
171 the accuracy of the algorithm with both mainstream and sidestream capnography.

172 *4.2. The capnogram based ventilation detector*

173 To date few capnogram based ventilation detectors applicable to OHCA data have been
174 described. However, the universalization of the capnogram during ALS and the importance of
175 adequate ventilation for the survival of the patient call for new and improved capnogram based
176 ventilation feedback algorithms. Our method relies on an adaptive thresholding to classify possible
177 ventilations detected in the first derivative (slope) of the capnogram. A preliminary version of the
178 method was previously described.²⁷ Edelson et al. proposed an adaptive CPR artefact suppressing
179 filter before detecting ventilations in the first derivative of the filtered signal and then used fixed
180 detection thresholds.²³ Adaptive filtering requires additional CPR-assist pad signals, such as depth,
181 acceleration and/or force signal. These signals need to be synchronized to the capnogram which is
182 often recorded by a different device. Edelson et al. reported SE/PPV of 82/91% respectively for
183 the ventilation detector, slightly below our results, and $> 80\%$ of the rate errors below $\pm 2 \text{ min}^{-1}$,
184 compared to the $> 90\%$ of our algorithm. As it can be observed in Fig. 4 the error of our
185 algorithm hardly increased for the intervals with CCs in the OHD, with LOAs close to 1.8 min^{-1} ;
186 the difference is higher in the IHD where the LOA is 1.5 min^{-1} in the intervals with CCs, and 0.5
187 min^{-1} for the complete dataset. This difference is attributable to the CC artefacts as well as to
188 the mechanical ventilations of the IHD .

189 Panels c and d of Fig. 4 show two cases where the algorithm was effective in the presence of
190 large CC artefacts. Panels a and b, are two exceptional cases that show the limitations of the
191 algorithm. Panel a corresponds to a ventilation technique leading to baselines too short to be
192 detected as true ventilations. Panel b shows a capnogram of a patient with airway obstruction,
193 due to bronchospasm, asthma or chronic obstructive pulmonary disease. In both cases the detector

194 missed most of the ventilations of the interval.

195 The artefacts in the capnogram due to CCs were visually identified in previous studies^{20,24} and
196 are frequent in OHCA episodes, 73.3% of the cases in the study by Idris et al.²² and 78.8% in
197 our study (37.6% of the ventilations). The severity of the artefact has not been characterized yet
198 and might vary with the position/depth of the CCs, the physiology of the patient, and probably
199 with the technology used to acquire. It is known that the sidestream capnography shows artifacts
200 and distortions that may appear as false disease waveforms,²⁶ and it might also show different
201 susceptibility to CC artifacts compared to mainstream capnography. A thorough research is needed
202 for a better understanding of the level, characteristics and differences of the CC artefact in both
203 capnography sampling techniques.

204 *4.3. Application scenarios*

205 Monitoring ventilation rate to avoid hyperventilation is a challenge in OHCA scenarios where
206 many feedback systems are available for CCs but not for ventilatory assistance. During BLS,
207 the impedance measured through defibrillation pads has been proposed to monitor ventilations.
208 Although impedance can be used for debriefing, it showed limited performance for monitoring
209 instantaneous ventilation rate. Alonso et al. reported significant errors due to non ventilatory
210 components of the impedance waveform,¹⁷ an observation consistent with the manual annotations
211 required in several studies on CPR quality.^{11,28} For ALS, where advance airway management is
212 integrated, the latest guidelines encourage the use of the capnogram to monitor CPR quality. Our
213 results show that ventilation rate algorithms should be further evaluated with capnograms acquired
214 during CCs before they are incorporated into feedback systems.

215 *4.4. Limitations*

216 The use of the algorithm is limited by the characteristics of the capnograms. As capnogram is
217 dependent on the perfusion and metabolism of the patient, for very low levels (< 5 mmHg in our
218 algorithm), ventilations would not be detected. The IHD used to test the algorithm is limited by
219 the number of episodes, 6 out of 21, which include CCs. Although few cases were available, the
220 inclusion of this dataset enabled the validation of the algorithm with a robust and independent
221 GS.

222 **5. Conclusions**

223 Our study proves that an accurate feedback on ventilation rate using only the capnogram is
224 feasible, even in intervals where the capnogram signal is severely corrupted by CCs. Technology
225 based on this type of algorithms could be integrated in monitor/defibrillators to provide reliable
226 feedback on ventilation rate and alarms on hyperventilation during CPR.

227 **Ethical Approval**

228 The CPR process files used in the OHD were collected as part of an effort to develop an airway
229 check algorithm using the capnogram. Since these raw data files have no identifying information,
230 the Institutional Review Board at the Oregon Health & Science University determined that the
231 proposed activity is not human subject research because the proposed activity does not meet the
232 definition of human subject per 45 CFR 46.102(f).

233 The files used in the IHD were collected as part of the investigation approved by the ethics
234 committee of the Medical University in Vienna. Subjects resuscitated successfully signed written
235 informed consent. For all others the Institutional Review Board waived the need for informed
236 consent. [<https://ekmeduniwien.at/core/catalog/2012> (EK-Nr: 1574/2012)]

237 **Conflict of interest**

238 Mohamud Daya is an unpaid consultant for Philips Healthcare.

239 **Acknowledgements**

240 This work received financial support from the Ministerio de Economía y Competitividad of
241 Spain through the projects TEC2012-31928 and TEC2015-64678-R, and from the University of
242 the Basque Country (UPV/EHU) through the unit UFI11/16. The Medical University of Vienna
243 received support in the form of a grant and the equipment used from Philips Healthcare, Bothell,
244 WA, USA.

- 245 [1] Soar J, Nolan JP, Böttiger BW, et al. European Resuscitation Council Guidelines for Resuscitation 2015.
246 Resuscitation 2015;95:100–147.
- 247 [2] Woodson RD. Physiological significance of oxygen dissociation curve shifts. Critical care medicine 1979;
248 7(9):368–373.
- 249 [3] Madden JA. The effect of carbon dioxide on cerebral arteries. Pharmacology & therapeutics 1993;59(2):229–250.
- 250 [4] Karlsson T, Stjernström EL, Stjernström H, Norln K, Wiklund L. Central and regional blood flow during
251 hyperventilation. An experimental study in the pig. Acta Anaesthesiologica Scandinavica 1994;38(2):180–186.
- 252 [5] Aufderheide TP, Sigurdsson G, Pirralo RG, et al. Hyperventilation-induced hypotension during
253 cardiopulmonary resuscitation. Circulation 2004;109(16):1960–1965.
- 254 [6] Aufderheide TP, Lurie KG. Death by hyperventilation: a common and life-threatening problem during
255 cardiopulmonary resuscitation. Critical Care Medicine 2004;32(9 Suppl):S345–351.
- 256 [7] O’Neill JF, Deakin CD. Do we hyperventilate cardiac arrest patients? Resuscitation 2007;73(1):82–85.
- 257 [8] Yannopoulos D, Tang W, Roussos C, Aufderheide TP, Idris AH, Lurie KG. Reducing ventilation frequency
258 during cardiopulmonary resuscitation in a porcine model of cardiac arrest. Respiratory Care 2005;50(5):628–635.
- 259 [9] Abella BS, Alvarado JP, Myklebust H, et al. Quality of cardiopulmonary resuscitation during in-hospital cardiac
260 arrest. JAMA 2005;293(3):305–310.
- 261 [10] McInnes AD, Sutton RM, Orioles A, et al. The first quantitative report of ventilation rate during in-hospital
262 resuscitation of older children and adolescents. Resuscitation 2011;82(8):1025–1029.
- 263 [11] Stecher FS, Olsen JA, Stickney RE, Wik L. Transthoracic impedance used to evaluate performance of
264 cardiopulmonary resuscitation during out of hospital cardiac arrest. Resuscitation 2008;79(3):432–437.
- 265 [12] Park SO, Shin DH, Baek KJ, et al. A clinical observational study analysing the factors associated with
266 hyperventilation during actual cardiopulmonary resuscitation in the emergency department. Resuscitation 2013;
267 84(3):298–303.
- 268 [13] Kramer-Johansen J, Edelson DP, Losert H, Köhler K, Abella BS. Uniform reporting of measured quality of
269 cardiopulmonary resuscitation (CPR). Resuscitation 2007;74(3):406–417.
- 270 [14] Hostler D, Everson-Stewart S, Rea TD, et al. Effect of real-time feedback during cardiopulmonary resuscitation
271 outside hospital: prospective, cluster-randomised trial. BMJ (Clinical research ed) 2011;342:d512.
- 272 [15] Aase SO, Myklebust H. Compression depth estimation for CPR quality assessment using DSP on accelerometer
273 signals. IEEE Transactions on Biomedical Engineering 2002;49(3):263–268.
- 274 [16] Ayala U, Eftestøl T, Alonso E, et al. Automatic detection of chest compressions for the assessment of
275 CPR-quality parameters. Resuscitation 2014;85(7):957–963.
- 276 [17] Alonso E, Ruiz J, Aramendi E, et al. Reliability and accuracy of the thoracic impedance signal for measuring
277 cardiopulmonary resuscitation quality metrics. Resuscitation 2015;88:28–34.
- 278 [18] Risdal M, Aase SO, Stavland M, Eftestøl T. Impedance-based ventilation detection during cardiopulmonary
279 resuscitation. IEEE transactions on bio-medical engineering 2007;54(12):2237–2245.
- 280 [19] Losert H, Risdal M, Sterz F, et al. Thoracic impedance changes measured via defibrillator pads can monitor
281 ventilation in critically ill patients and during cardiopulmonary resuscitation. Critical Care Medicine 2006;
282 34(9):2399–2405.

- 283 [20] Daya MR, Idris AH, Helfenbein ED, Babaeizadeh S, Zhou S, Zive D. Abstract 237: Assessment of Airway
284 Placement During Out-of-Hospital Cardiac Arrest Using an Automated Capnogram Analysis Algorithm.
285 *Circulation* 2010;122(Suppl 21):A237–A237.
- 286 [21] Daya M, Helfenbein E, Idris A, et al. Abstract 84: Hyperventilation Alert During Out-of-Hospital
287 Cardiopulmonary Resuscitation Using an Automated Capnogram Analysis Algorithm. *Circulation* 2011;124(21
288 Supplement):A84.
- 289 [22] Idris AH, Daya M, Owens P, et al. Abstract 83: High Incidence of Chest Compression Oscillations
290 Associated With Capnography During Out-of-Hospital Cardiopulmonary Resuscitation. *Circulation* 2010;122(21
291 Supplement):A83.
- 292 [23] Edelson DP, Eilevstjønn J, Weidman EK, Retzer E, Hoek TLV, Abella BS. Capnography and chest-wall
293 impedance algorithms for ventilation detection during cardiopulmonary resuscitation. *Resuscitation* 2010;
294 81(3):317–322.
- 295 [24] Aramendi E, Alonso E, Russell JK, Daya M, Gonzalez-Otero D, Ayala U. Monitoring respiratory rate with
296 capnography during cardiopulmonary resuscitation. *Resuscitation* 2014;85, Supplement 1:S26–S27.
- 297 [25] Jaffe MB. Mainstream or sidestream capnography? *Respironics, Inc* 2002;4:5.
- 298 [26] Pascucci RC, Schena JA, Thompson JE. Comparison of a sidestream and mainstream capnometer in infants.
299 *Critical care medicine* 1989;17(6):560–562.
- 300 [27] Elola A, Chicote B, Aramendi E, et al. A method to measure ventilation rate during cardiopulmonary
301 resuscitation using the capnogram. In *Computing in Cardiology Conference (CinC)*, 2015. 2015, 1001–1004.
- 302 [28] Idris AH, Beadle S, Daya M, Zive D. Abstract P101: Comparison of Ventilation Rate Measured with Thoracic
303 Bioimpedance and with Capnography during Out-of-Hospital Cardiopulmonary Resuscitation. *Circulation* 2008;
304 118(Suppl 18):S_1467–S_1467.

305 Figure Legends

- 306 Figure 1 Intervals from the out-of-hospital and in-hospital datasets, OHD and
307 IHD, showing the capnogram and the Gold Standard (GS) to annotate
308 ventilations. Panels a and b show OHD examples without and with
309 chest compressions, with the impedance ventilation channel (GS) in
310 black on top and the capnogram below. Panels c and d show IHD
311 examples without and with CCs, with the air volume (GS) on top
312 and the capnogram below.
- 313 Figure 2 The four phases of the normal capnogram and the features of the
314 ventilation detector associated to potential ventilation number k .
315 The time stamps $t_{insp,k}$ and $t_{exp,k}$ correspond to the inspiration and
316 expiration times respectively.
- 317 Figure 3 Box plots showing the performance of the ventilation detector for
318 the out-of-hospital dataset, OHD, in panel a, and for the in-hospital
319 dataset, IHD, in panel b. Results are also given for the intervals with
320 chest compressions (CCs).
- 321 Figure 4 Performance of the ventilation detection algorithm with four episodes.
322 The examples of panels a, b and c correspond to episodes from the
323 out-of-hospital dataset, and example of panel d to an episode from
324 the in-hospital dataset. For every example the gold standard (GS) is
325 shown (impedance ventilation signal or air flow volume signal). The
326 GS annotations are shown with black dashed lines, and the detected
327 ventilations with red triangles.
- 328 Figure 5 Bland-Altman plots for the out-of-hospital and in-hospital datasets,
329 OHD and IHD respectively, for all cases and for the intervals with
330 chest compressions. The horizontal lines show the 95% level of
331 agreement.

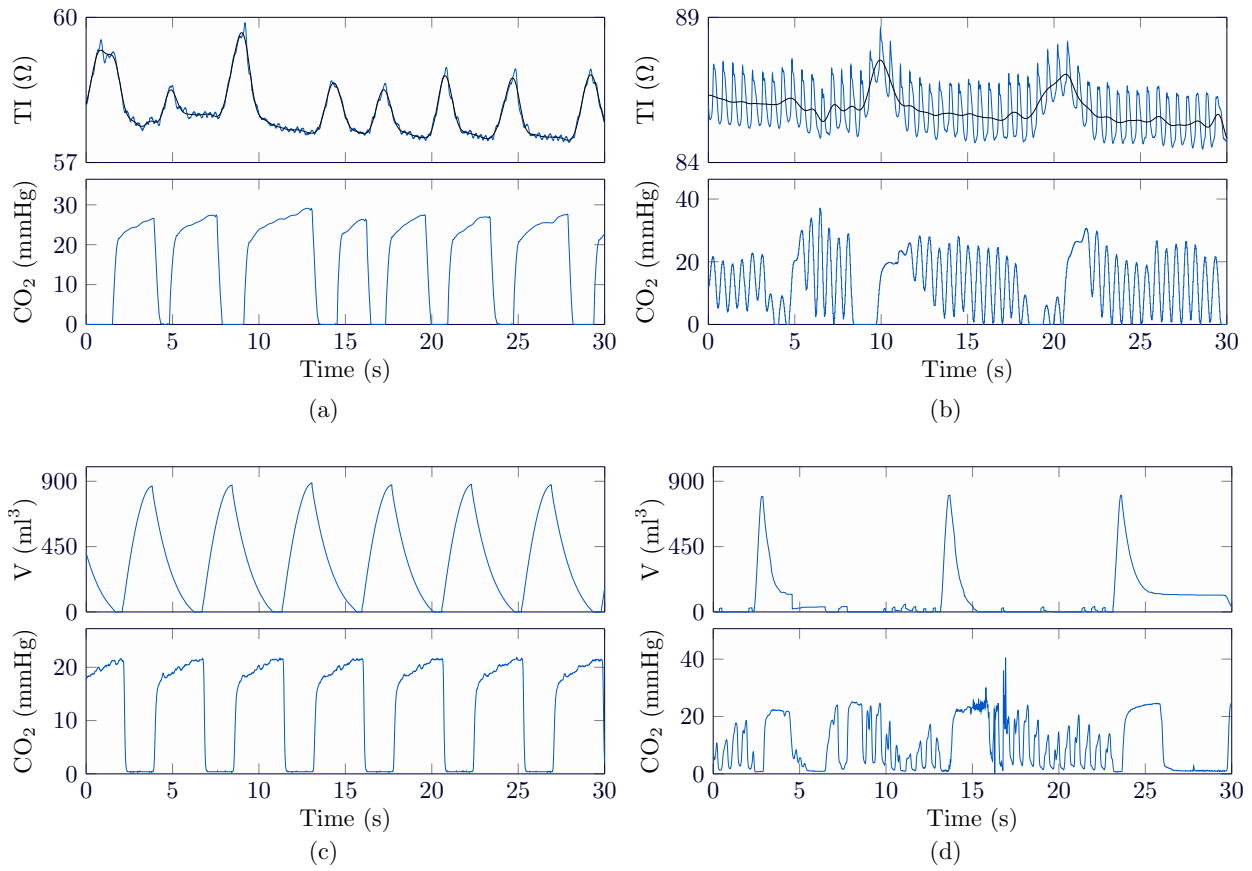


Figure 1: Intervals from the out-of-hospital and in-hospital datasets, OHD and IHD, showing the capnogram and the Gold Standard (GS) to annotate ventilations. Panels a and b show OHD examples without and with chest compressions, with the impedance ventilation channel (GS) in black on top and the capnogram below. Panels c and d show IHD examples without and with CCs, with the air volume (GS) on top and the capnogram below.

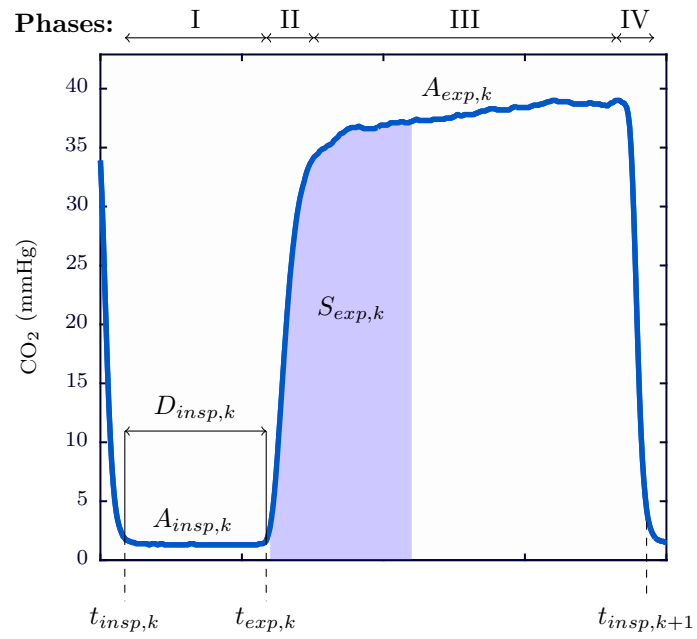
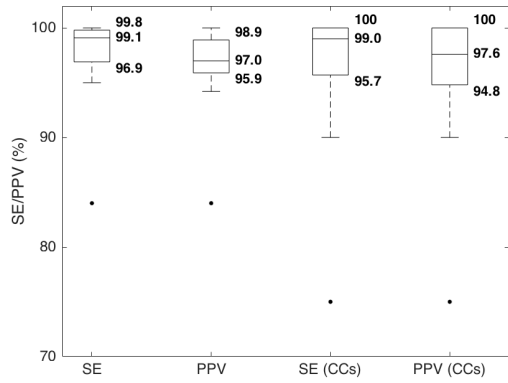
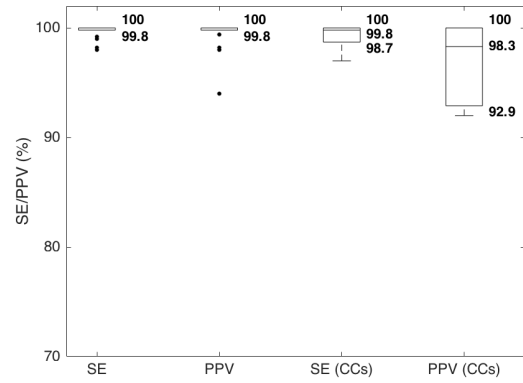


Figure 2: The four phases of the normal capnogram and the features of the ventilation detector associated to potential ventilation number k . The time stamps $t_{insp,k}$ and $t_{exp,k}$ correspond to the inspiration and expiration times respectively.



(a) OHD all cases and during CCs



(b) IHD all cases and during CCs

Figure 3: Box plots showing the performance of the ventilation detector for the out-of-hospital dataset, OHD, in panel a, and for the in-hospital dataset, IHD, in panel b. Results are also given for the intervals with chest compressions (CCs).

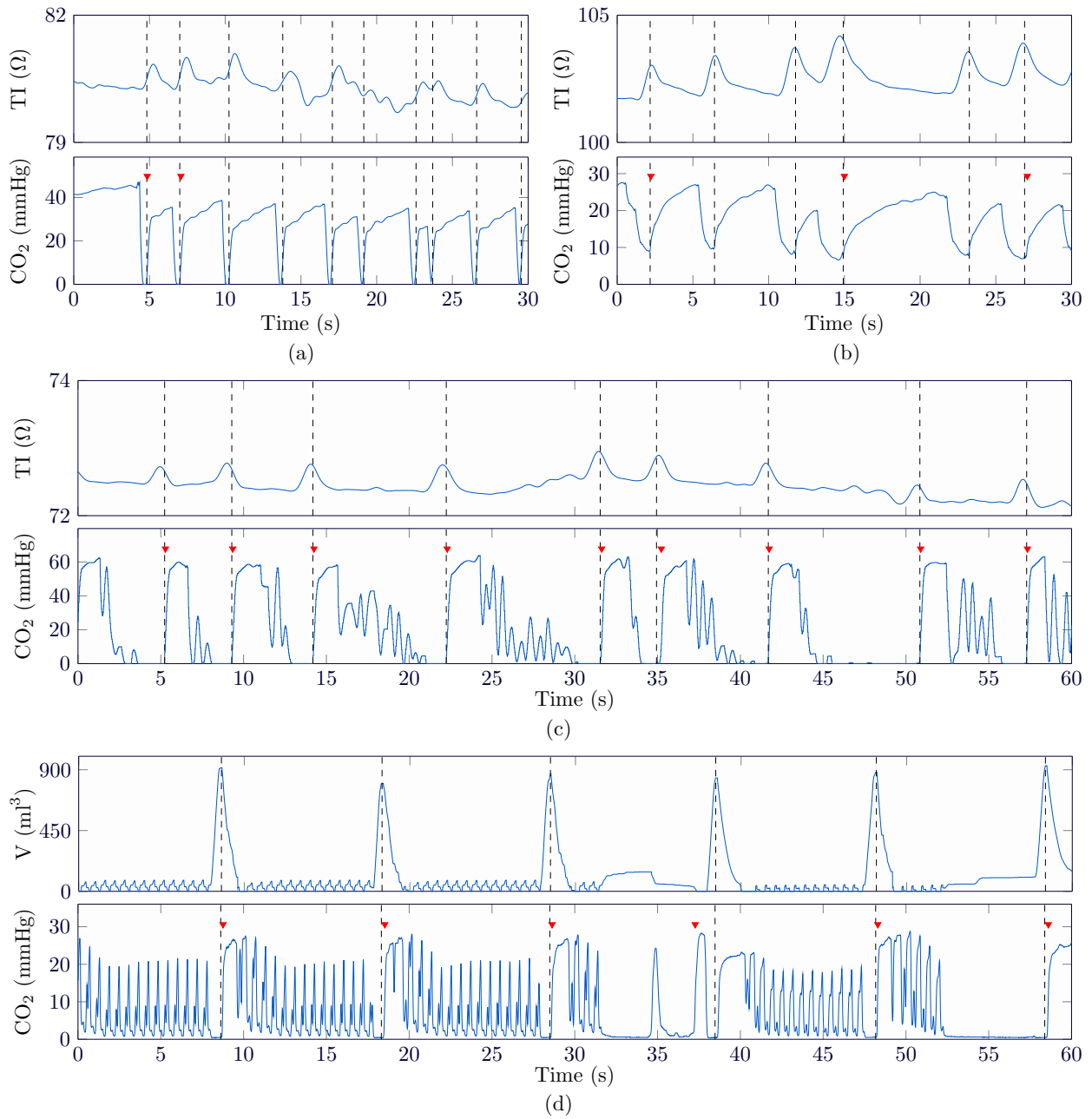


Figure 4: Performance of the ventilation detection algorithm with four episodes. The examples of panels a, b and c correspond to episodes from the out-of-hospital dataset, and example of panel d to an episode from the in-hospital dataset. For every example the gold standard (GS) is shown (impedance ventilation signal or air flow volume signal). The GS annotations are shown with black dashed lines, and the detected ventilations with red triangles.

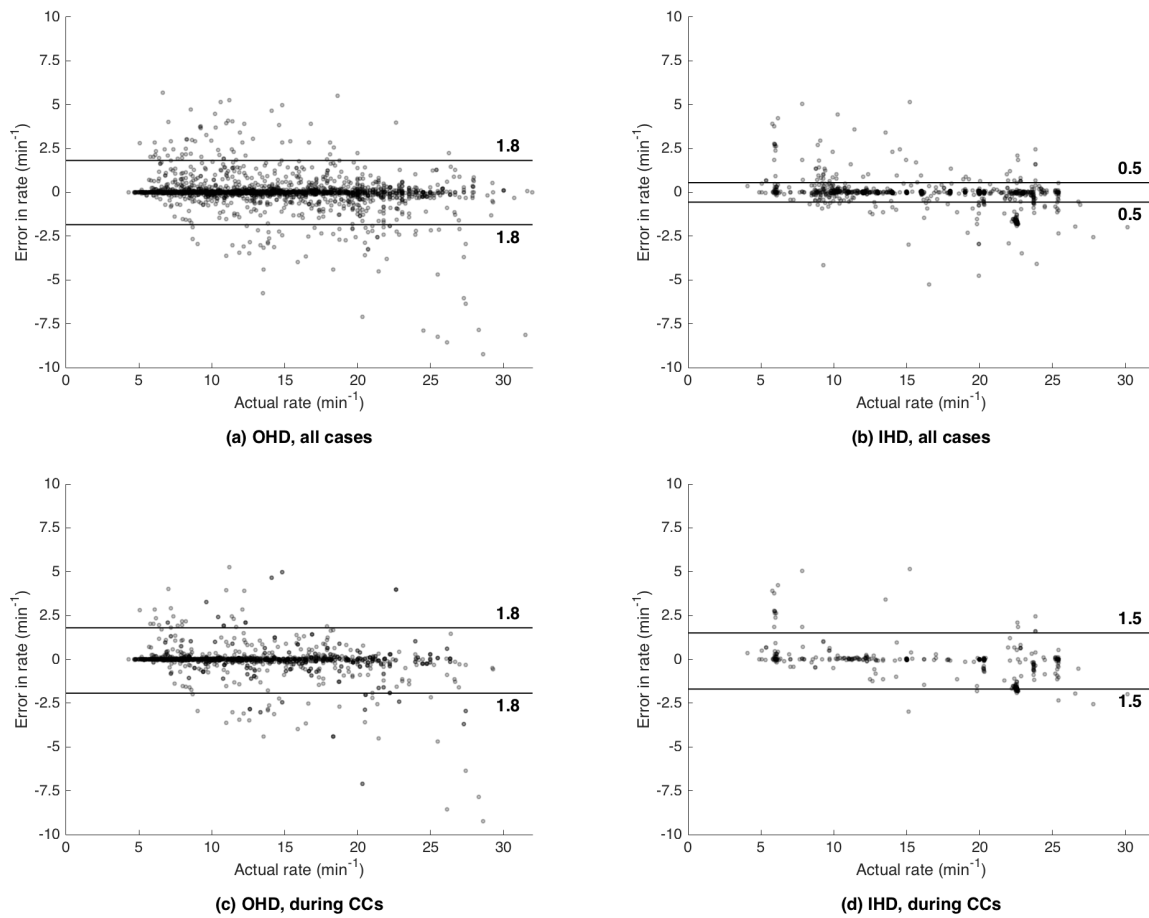


Figure 5: Bland-Altman plots for the out-of-hospital and in-hospital datasets, OHD and IHD respectively, for all cases and for the intervals with chest compressions. The horizontal lines show the 95% level of agreement.

332 **Table Legends**

333 Table 1 Characteristics of the out-of-hospital dataset (OHD) and the in-hospital
334 dataset (IHD)

Parameter	OHD	IHD
Number of episodes	62	21
Total duration (min)	2545	2335
Total number of ventilations (% with CPR)	16899 (37.6)	29841 (8)
Instantaneous ventilation rate (min^{-1})	10 (8.7-13.1)	14.3 (12.6-18.2)
Minutes with hyperventilation per episode (%)	10 (2-35)	14 (0-88)

Table 1: Characteristics of the out-of-hospital dataset (OHD) and the in-hospital dataset (IHD)